Effect of interfacial defect on surface crack behavior of an air plasma sprayed thermal barrier coating

Xu Rong, Zhang Weixu, Fan Xueling, Wang Tiejun*

State Key Laboratory for Strength and Vibration of Mechanical Structures, School of Aerospace Engineering, Xi'an Jiaotong University, Xi'an 710049, China
* Corresponding author: wangtj@mail.xjtu.edu.cn

Abstract Multiple surface cracking has significant effect on the failure of thermal barrier coating system (TBCs). The surface cracking is influenced by interface defects. It is of significance to study the relationship between the interface defect and the surface crack. In present work, the effect of interface defect on the surface crack behavior of TBCs has been investigated by using finite element method. The strain energy release rate (SERR) of the surface vertical crack is obtained as functions of the interfacial defect length and location. The results show that both the defect location and the defect length have a significant influence on the driving force of surface crack. It is concluded that the interface defect under the surface crack may induce a more intense facilitation on the surface cracking behavior than the remote defect. Moreover, a large scale interface defect may also induce a larger SERR of the surface crack which may promote its propagation.

Keywords Thermal barrier coating, Surface crack, Interfacial delamination, Strain energy release rate

1. Introduction

Thermal barrier coating systems (TBCs) are widely used in gas turbines or diesel engines due to their excellent heat-insulating property, which can efficiently prolong the life of the turbines blades[1, 2]. The major role contributing to the heat-insulating is the top layer of the TBCs, a ceramic coat with low thermal conductivity, which provides a temperature reduction of the metallic substrate[3, 4]. In order to protect the substrate from oxidation and make a better bond strength of the top coat to the substrate, a metallic bond coat is deposited between the top coat and the substrate. The top ceramic coat, metallic bond coat and substrate build up the typical TBCs.

Due to the mismatch of the geometric dimensions and the material properties, some fracture phenomena are inevitable in the TBCs[5, 6]. The common fracture behaviors observed during the service are the multiple surface cracks and the interface cracks[7, 8]. Considerable work was focused on the surface cracking behavior in the film/substrate system. Schulze and Erdogan[9] analyzed the periodic cracking of an elastic coating bonded to a homogeneous substrate. Vlassak[10] studied the channel cracking in thin films on substrates of finite thickness in order to simulate the segmentation of the ceramic layer of TBCs. Recently, by using finite element method, Fan *et al*.[11, 12] and Zhang *et al*.[13] built a three-layer model to investigate the effects of several important characteristic parameters, e.g. the interface roughness, thermally grown oxide (TGO), etc., on the periodic surface crack behavior. However, it is assumed in most of the aforementioned investigations that the ceramic/bond coat interface of TBCs is perfect, which ignores the fact that interface cracks may be initiated due to stress concentration.

The interface cracks have been frequently observed during the service, which lead to the spalling of ceramic coating and eventual failure of TBCs. The analyses and explanations for the appearances of interface cracks were presented by many researchers. Rice[14] developed the elastic fracture mechanics concepts for interfacial cracks between dissimilar solids, which made a great contribution to the interface cracks analysis in TBCs. Mumm and Evans[15] focused on the interface crack induced by the TGO growth. In their study, the morphological imperfections in the TGO played a great role in the failure of TBCs. Another significant reason for the initiation of interface cracks is the natural restrictions of depositing process especially the air plasma spraying. Currently, it is generally accepted that the ceramic coating of air plasma spraying TBCs exhibits laminar structural characteristic. Pores and micro-cracks are inevitable due to the internal thermal

stress in the process of thermal spraying[16-18]. The defects near the interface may coalesce during the service, leading to the interface cracks[19, 20].

The original motivate of present work is the author's experiment observations to TBCs that the surface cracks intensively appears in some areas of the ceramic coating of TBCs. Generally, one reason for the phenomenon is that, after air plasma spraying, as previous mentions, the ceramic/bond coat interface usually contains numbers of small scale delamination, which may promote the surface crack emerging above it. Another one is that the facilitation of the interfacial delamination induced by TGO growth or material property mismatch to the surface cracks. In general, the interaction between the interface defect and surface rupture make a great contribution to the experiment observations. In order to understand the fracture mechanisms of the TBCs clearly, the analyses of the mutual effects between the interface defect and surface rupture should be extremely necessary. More recently, investigations focus on the interaction of interfacial delamination and surface cracks[21, 22]. Among these studies, much attention has been paid on the effect of the surface cracks on the interfacial delamination, the basic assumption of which is that the interfacial delamination initiated from roots of surface channel cracks. However, for most cases, the interface cracks exist before the top ceramic coating starts to failure. Therefore, it is important to investigate the effect of the pre-existing interfacial defect on the ceramic failure especially on the initiation and propagation of the surface vertical crack. Zhou and Kokini[21] investigated the effect of pre-existing surface crack morphology on the interfacial thermal fracture and demonstrated that the large density of the period surface cracks can postpone the interfacial delamination, Fan *et al*. [22] used FEM to obtain the critical spacing of the periodic surface cracking below which the surface channel cracks have a dramatic effect on the interfacial delamination. However, much less attention has been paid directly to the effect of interface defect on the coating rupturing. In practice, actual spalling failure of TBC is followed by multiple surface cracks that propagate through the top coat and coalesce with interfacial crack between the top coat and the bond coat[22]. Therefore, to design excellent TBCs with high durability, it is necessary to study the effect of the interface cracks on the surface cracks which determines the coalescent of the surface cracks and interface cracks. In this paper, we build a multiple-layers TBCs model which contains pre-existing interfacial defect to investigate the effect of pre-existing interfacial defect on surface cracking. In Section 2, we firstly descript the numerical model for the problem of surface cracks and interfacial defect in TBCs. In Section 3, the crack driving forces for surface cracks are calculated, and moreover the effect of interfacial defect on surface cracks is discussed in detail. Section 4 summarizes the concluding remarks and emphasizes the effect of interfacial cracks on the durability of TBC system.

2. Statement of the problem

Due to the pre-existing interfacial defect after air plasma spraying or the interface cracks induced by thermal stress, the interfacial delamination probably emerges in some small areas, which effects the inevitable following surface cracks and the subsequent coalescent of the surface cracks and interface cracks. A steady state concept for cracks in multilayer structure is essential for many situations, where the crack driving force of surface crack is independent of the tunnel length if the length is enough long. Once the steady state is reached, the crack driving force can be calculated by using a two-dimensional (2D) plane strain model[23]. As a result, a three-dimensional TBCs model with surface cracks and interface defects is reduced to a 2D plane stain model. Fig. 1 shows the 2D plane strain model of steady state multiple surface cracks accompanied with interfacial cracks, in which h, a and W are the ceramic coating thickness, the surface crack length, and the cell model width, respectively. Based on our experimental observation[22], when the distance between adjacent surface cracks is large enough (about ten to twenty times the film thickness), the interaction between neighboring surface cracks can be ignored. Therefore, a unit cell model with single surface crack and interfacial defect can be constructed to simulate the actual TBCs with multiple cracks by setting the W equal twenty times the ceramic coating thickness.

The coordinate system (x, y) is set at the top surface of the film with surface crack, whose length a is along to y-axis. An interface defect with length l is presetting at the top/bond coating interface, the center of which offsets from the y-direction by c.

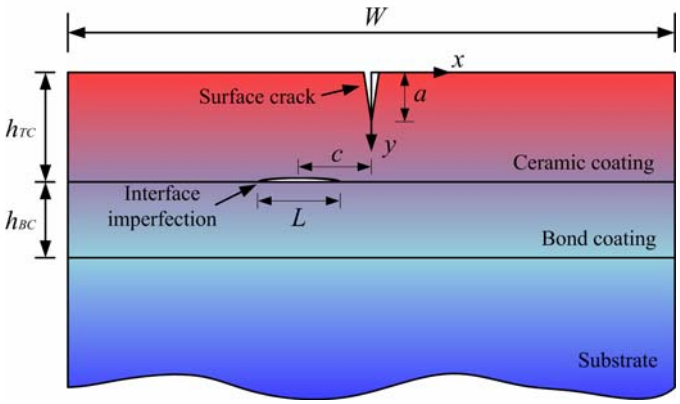

Figure 1. The TBCs model with surface crack in the TC and interfacial crack at TC/BC interface.

Assume a uniform strain is remotely applied to the TBCs system in the x-direction, the remote stress in the top coating is given by

$$\sigma_0 = \frac{\varepsilon_0 E_1}{1-\upsilon_1^2} \tag{1}$$

where E_1, υ_1 are the Young's modulus and Poisson's ratio of top coating. Therefore, the mixed boundary conditions on the surface crack faces can be expressed as

$$\begin{cases} \sigma_{ij}(0,y) = 0, & 0 < y < a \\ u_i(0+0,y) = u_i(0-0,y), & a < y < h \end{cases} \tag{2}$$

where σ_{ij} (i,j=x,y) is the stress component and u_i (i,j=x,y) is the displacement in x-direction or y-direction, respectively.

Moreover, the stress on the interface crack face at interfacial delamination area should be zero and in other area at the interface the displacement should be continuous. The mixed boundary conditions at the interface are shown as

$$\begin{cases} \sigma_{ij}(x,h) = 0, & -c-\dfrac{l}{2} < x < -c+\dfrac{l}{2} \\ u_i(x,h-0) = u_i(x,h+0), & x < -c-\dfrac{l}{2} \text{ and } x > -c+\dfrac{l}{2} \end{cases} \tag{3}$$

The problem can be solved by the superposition technique. The film/substrate system without any cracks is solved first and then added the stresses to the crack faces to represent the applied external loads σ_0. Then the numerical solution for mode I stress intensity factor (SIF) of the surface crack in a film/substrate system without any interfacial defect has been given by Beuth[24]

$$K/\sigma_0\sqrt{h} = 1.1215\sqrt{\pi}\left(a/h\right)^{1/2}\left(1-a/h\right)^{1/2-s}\left(1+\lambda a/h\right) \tag{4}$$

where the λ is a curve fitting parameter which is dependent of a/h, The value of λ also been given by Beuth[24]. The s is the singularity exponent which depends on elastic mismatch, and is the root to

$$\cos(s\pi) - 2\frac{\alpha-\beta}{1-\beta}(1-s)^2 + \frac{\alpha-\beta^2}{1-\beta^2} = 0 \tag{5}$$

where α, β are two non-dimensional Dundurs' parameters representing the material mismatch between adjacent layers[25]. For the plane strain problem, the Dundurs' parameters α, β can be

expressed as

$$\alpha = \frac{\bar{E}_1 - \bar{E}_2}{\bar{E}_1 + \bar{E}_2} \tag{6}$$

$$\beta = \frac{1}{2}\frac{\mu_1(1-2\upsilon_2) - \mu_2(1-2\upsilon_1)}{\mu_1(1-\upsilon_2) - \mu_2(1-\upsilon_1)} \tag{7}$$

where $\bar{E}_i = E_i / \left(1 - v_i^2\right)$, E_i, υ_1 and μ_1 are the plane strain modulus, Young's modulus, Poisson's ratio, and shear modulus of film/substrate systems' components, respectively. For homogeneous materials, the Dundurs' parameters are written as $\alpha = \beta = 0$.

Strain energy release rate (SERR) is another basic concept to study the driving force of an crack. A larger SERR value of the surface crack tip presents the more probability of surface rupturing. The SERR can be calculated by SIF and the Young's modulus of the top coating

$$G = \frac{K^2}{\bar{E}} \tag{8}$$

In present work, the multiple layers TBCs model with pre-existing interface crack has tiny differences with the typical film/substrate system. In detail, the interfacial defect existence may make it difficult to investigate the fracture mechanism in TBCs by using classical fracture mechanism. Fortunately, the finite element method can calculate the value of SIF and SERR accurately. Therefore, the commercial soft ABAQUS is adopted in present work to obtain the effect of the interfacial defect on the surface crack driving force (e.g. SERR). In the preliminary calculation, we found that a relatively small interfacial defect has little influence on the crack mode. In general, the mode II SIF is less than one-tenth of the mode I SIF, which means that the mode I crack dominates the fracture behavior and mode II crack can be ignored in the following analyses. Therefore, the SERR for the surface crack can be written in a similar form with Eq. (4)

$$K / \sigma\sqrt{h} = w(\alpha, \beta, \bar{a}, \bar{L}, \bar{c}) = \eta(\alpha, \beta, \bar{a}, \bar{L}, \bar{c})\bar{w}(\alpha, \beta, \bar{a}) \tag{9}$$

where the function w is the value of normalized SIF of surface crack obtained by FEM, and $\bar{w}$ represents the right expression of Eq. (4), which is determined by the Dundurs' parameters α, β and surface crack length $\bar{a} = a / h$. The revised function η is regarded as the function of the interface crack geometric characteristic, the crack length $\bar{L} = L / W$ and the crack location $\bar{c} = c / W$. Similarly, the SERR can also be written as follow by using the Eq. (8) and Eq. (9)

$$\frac{G\bar{E}}{\sigma^2 h} = Z(\alpha, \beta, \bar{a}, \bar{L}, \bar{c}) = \kappa(\alpha, \beta, \bar{a}, \bar{L}, \bar{c})\bar{Z}(\alpha, \beta, \bar{a}) \tag{10}$$

where the function Z, κ and $\bar{Z}$ represent the SERR value function, the revised function of the interfacial defect and the original SERR function without interfacial defect, respectively.

Since it is intractable to calculate SIF and SERR for an crack in TBCs, the more convenient calculation of SERR is applied in this paper. In the linear elastic fracture mechanics, the SIF and the SERR can be represented by the value of J-integral. Therefore, SERR associated with crack length can be calculated by J-integral method. For a virtual crack advance $\lambda(s)$, the value of J-integral can be calculated by [26]

$$\bar{J} = \int_A \lambda(s)\mathbf{n} \cdot \mathbf{H} \cdot \mathbf{q} dA \tag{11}$$

where dA is the total areas of a layer of elements enclosing the crack tip, $\mathbf{n}$ is the outward normal vector to the corresponding integral contour, and $\mathbf{q}$ is the direction of virtual crack extension, $\mathbf{H}$ is given by

$$\mathbf{H} = \left(W\mathbf{I} - \boldsymbol{\sigma} \cdot \frac{\partial \mathbf{u}}{\partial \mathbf{x}} \right) \tag{12}$$

where W is strain energy.

The finite element code ABAQUS is employed for numerical calculations. A fine mesh near

the crack tip is necessary for the regular finite element method in the typical TBCs model. Eight-node bilinear plane strain quadrilateral reduced integration elements are selected for all three layers except the crack tip region, where very fine mesh of singular elements are constructed. In addition, The J contour integral values are independent to the mesh configuration if the mesh configuration is fine enough around the crack tip. Herein, each layer in TBC is taken to be homogeneous, isotropic and linear elastic materials whose geometry and material properties are $h = h_{TC} = 0.2$ mm , $h_{BC} = 0.1$ mm , $h_S = 30$ mm , $E_{TC} = 60$ GPa , $E_{BC} = 200$ GPa , $E_S = 211$ GPa , $\nu_S = \nu_{BC} = \nu_{TC} = 0.3$ and $W / h = 20$, where the subscripts TC, BC and S represent top coat, bond coat and substrate, respectively.

3. Result and Discussion

In fracture mechanics, SERR at the crack tip can regarded as the driving force of the crack. Therefore, obtaining the SERR value of the surface crack for different lengths can detailedly describe the initiation and propagation of it. Fig.2 shows reduced revised function $\kappa(\bar{a},\bar{L},\bar{c})$ as a function of interfacial defect location for different surface crack length. Noted that the length of presetting interface crack is fixed as a uniform value $\bar{L} = 0.15$ in order to investigate the separate effect of interface crack location on the driving force of surface crack. As discussed earlier, the SERR for the surface crack in the TBCs with interface defect can be written as Eq. (10) which consist two functions, the revised function and the original SERR function without interface defect, respectively. In Fig.2, the value of $Z(\alpha,\beta,\bar{a},\bar{L},\bar{c}) / \bar{Z}(\alpha,\beta,\bar{a})$ in Eq. (10) for a constant $\bar{L} = 0.15$ equals to the normalized SERR $G / \bar{G}$. Therefore, the reduced revised function $\kappa(\bar{a},\bar{L},\bar{c})$ (α,β is constant since the material parameter is uniform) for $\bar{L} = 0.15$ can be obtained from the normalized SERR. The $\kappa(\bar{a},\bar{L},\bar{c})$ for $\bar{L} = 0.15$ is always larger than 1 for all surface crack length, a / h , which means the interface defect always promotes the initiation and propagation. This promotion is the result of the constrain reducing for the top coating caused by the interface defect. The close analyses have also been made by Tsui *et al.*[27] and Thouless *et al.*[28].

Noted that the $\kappa(\bar{a},\bar{L},\bar{c})$ curve for small a / h slightly deviates from the dash line standing for the SERR function without interface defect $\bar{Z}(\alpha,\beta,\bar{a})$ while the $\kappa(\bar{a},\bar{L},\bar{c})$ for relatively large a / h is much bigger ,which means that the interface defect effects the propagation of the surface crack more dramatically than the initiation. That's to say, the initiation of the surface crack appears to be impendent on the interface defect offset while the propagation intensively depend on the interface defect location. In addition, when the surface crack approach to the interface, the $\kappa(\bar{a},\bar{L},\bar{c})$ seems to decrease slightly (i.e. the curves for a / h =0.8 or 0.9 is in a low degree compared to that for a / h =0.6 or 0.7).

As shown in Fig.2, the interface defect offset $\bar{c}$ is a significant factor to affect the propagation of the surface crack. For the large offset $\bar{c}$, the $\kappa(\bar{a},\bar{L},\bar{c})$ is approach to 1, indicating the variation of SERR is exactly similar to the solution for perfect interface. Therefore, in this case, the remote interface defect appears to have relatively little influence on the surface cracking behavior. Conversely, when the offset is equal to zero, the $\kappa(\bar{a},\bar{L},\bar{c})$ seems to largely deviate from the dash line(i.e. the solution for perfect interface). In other words, the interface defect under the surface crack may promote the surface crack propagation more vigorously than the remote one. As a result, the surface cracks centralizing in some areas under of which there exists potential interface cracks may propagate much faster. Then they easily penetrate into the interface and coalesce with the interface cracks, which lead the eventual spalling of the ceramic coating. Therefore, we consider the interface defect as a significant reason for the premature failure of TBCs during service.

As the absolute value of $\bar{c}$ enlarges to a critical value, the $\kappa(\bar{a},\bar{L},\bar{c})$ for $\bar{L} = 0.15$ becomes

asymptotic to 1. Therefore, $Z(\alpha,\beta,\bar{a},\bar{L},\bar{c})$ seems to approach to $\bar{Z}(\alpha,\beta,\bar{a})$ which indicates the influence of interface can be ignored. In present model, the critical offset value is about 0.15 above which the interaction between surface crack and interface defect can be ignored. Moreover, a interesting finding in Fig.2 is that the $\kappa(\bar{a},\bar{L},\bar{c})$ for $a/h=$ 0.8 and 0.9 exhibits an irregular convex at $\bar{c}=\pm 0.05$. This irregular effect on surface cracking behavior is related to the extra deviating driving force induced by an asymmetric loading and restraint which are a result of the offsetting interface defect. Next part we will discuss this irregular behavior.

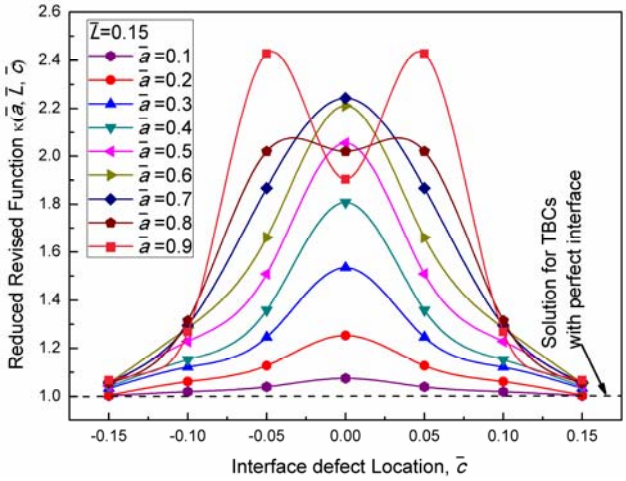

Figure 2. The reduced revised function $\kappa(\bar{a},\bar{L},\bar{c})$ as a function of interface defect location for different surface crack length.

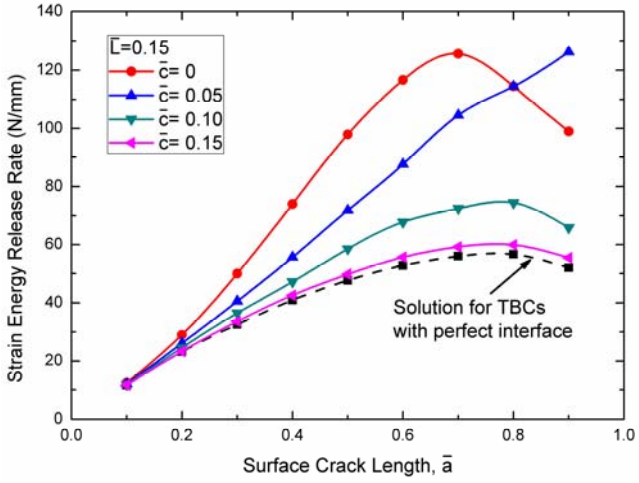

Figure 3. The SERR as a function of surface crack length for different interface defect offset.

Figure 3 shows the variations of SERR with normalized crack length a/h for the different offset of the interfacial defect. Moreover, SERR for the TBCs model with perfect interface is also plotted in Figure 3 for comparing. It is seen that the SERR for perfect interface rises to the maximum value as surface crack propagates and then drops as the crack approaches to interface, which coincides with the results obtained by Beuth[24]. Moreover, it is interesting to find that the overall trend of SERR curve in Figure 3 would change as the offset decrease. For the remote defect (e.g. $\bar{c}=0.15$), the curve of is much similar to the solution for perfect interface which, as previous described, rises to the maximum value as surface crack propagates and then drops as the crack approaches to interface. However, when the defect offset diminishes to 0.05, the SERR curve turns to monotonously ascend (e.g. $\bar{c}=0.05$). Then, Continue to decrease the offset of the defect, the

oscillation of SERR curve appears again (e.g. $\bar{c} = 0$) and the SERR reduces to a relatively low value. This behavior seems to be a result of the asymmetric loading and restraint causing by the offset of interface defect. An asymmetric loading and restraint may induce the extra deviating force for the surface crack. Therefore, the driving force would continue to increase instead of dropping as the crack approaches to interface, which may facilitate the deviation of the surface crack when it approaches to interface. Obviously, it can explain why the SERR curve for $a/h =$ 0.8 and 0.9 exhibit irregular convex at $\bar{c} = \pm 0.05$.Interestingly, this deviation has been observed by present researchers in their experiments[6]. If the defect is remote from the surface crack, its influence on surface crack is much small so that the deviating force is inconspicuous. Therefore, for the remote defect (e.g. $\bar{c} = 0.15$), the curve of SERR do not appear monotonous increasing.

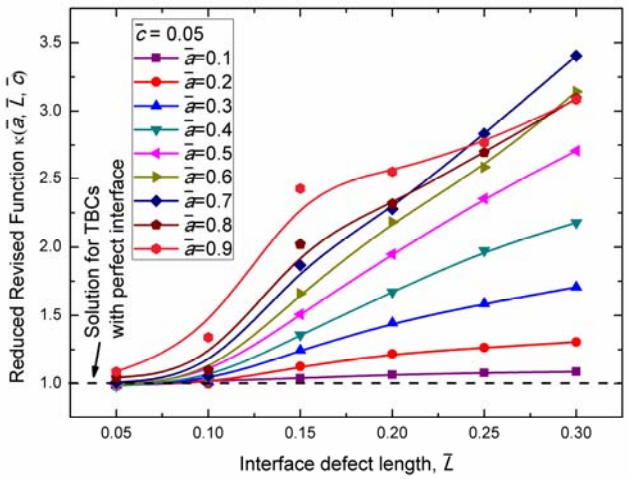

Figure 4. The reduced revised function $\kappa(\bar{a}, \bar{L}, \bar{c})$ as a function of interface defect length for different surface crack length.

The reduced revised function $\kappa(\bar{a}, \bar{L}, \bar{c})$ as a function of normalized surface crack length for different interfacial defect length is plotted in Fig. 4. In present figure, the interface defect offset $\bar{c}$ has been fixed as 0.05 and the surface crack length has been enlarged in order to simulate the spread of interface defect during the service of TBCs. Since the interface defect location has been fixed, the altering of $\kappa(\bar{a}, \bar{L}, \bar{c})$, which is obtained, as mentioned earlier, by the normalized SERR, can separately demonstrate the effect of defect length. In Fig. 4, it is seen that interfacial defect length is also a significant factor that affects the surface crack driving force.

For a small interface defect, the interface defect seems to have little influence to the surface crack. Noted that when the $\bar{L}$ is about 0.05, the value of SERR is close to the solution for perfect interface (the dash line in Fig. 4), which indicates that there may be an asymptotic curve for very low values of interface defect length. In other words, in present model, when the normalized length of interface defect with offset $\bar{c} = 0.05$ is smaller than 0.05, the interface can be regarded as a perfect one. For a relatively large interface defect, the value of $\kappa(\bar{a}, \bar{L}, \bar{c})$ rises to a high degree. For example, when the surface crack propagates about seventy percent of the ceramic coating, the $\kappa(\bar{a}, \bar{L}, \bar{c})$ for the $\bar{L} = 0.3$ is about 3.3, which indicate an interface defect with a length $\bar{L} = 0.3$ would make the driving force of surface crack more than three times larger since the substrate restrain is greatly reduced due to the interface defect. Obviously, the facilitation of the large scale interface defect may induce the premature coalescent of the surface crack and the interface crack, which contributes to the spalling of the ceramic coating. Therefore, a well bonded interface should be ensured in order to enhance the durability of the TBCs.

Compared to the Fig. 2, it seems that the effect of lengthening the interface defect length on the surface crack driving force is very similar to the effect of diminishing the offset of the interface

defect. They both promote the propagation of surface crack dramatically. Interestingly, as the interface defect length enlarges, the transformation of the SERR curves from oscillation (e.g. $\overline{L}=0.05$) to monotone (e.g. $\overline{L}=0.15$) and then back to oscillation (e.g. $\overline{L}=0.25$), which, as previous discussed, is induced by the extra deviating force, can also been found in Fig. 4.

As discussed above, it is concluded that the interface defect would promote the surface cracking behavior by increasing the SERR around the crack tip. Herein, it is generally accepted that the maximum increment of SERR induced by the interface defect is critical to estimate emanation of surface crack. Fig. 5 shows the maximum normalized SERR increment as a function of interfacial defect length and location. Two most important characteristics of interface defect, the length and the location, have been taken into consideration to investigate the their combined effect on surface crack. As shown in Fig. 5, the maximum normalized SERR increment for a remote interface defect ($\overline{c}=0.15$) is near to zero for a relatively small critical defect length (e.g. when $\overline{L}$ is less than 0.15), which means the remote and small defect has less potential to affect the surface cracking behavior. However, when interface defect is closer to the surface crack(e.g. $\overline{c}=0.05$), the critical defect length below which the defect can be ignored correspondingly decreases (e.g. $\overline{L}$ is less than 0.05). The most extreme situation is that the interface defect locates under the surface crack, in which the small defect cannot be ignored (as the black line in Fig. 5). In general, the maximum normalized SERR increment for a central interface defect is higher than the counterpart for the offsetting defect excepted the appearance of the extra deviating force for the surface crack, as discussed earlier, induced by asymmetric loading and restraint. The oscillation of the maximum normalized SERR increment curve stands for the extra deviating force.

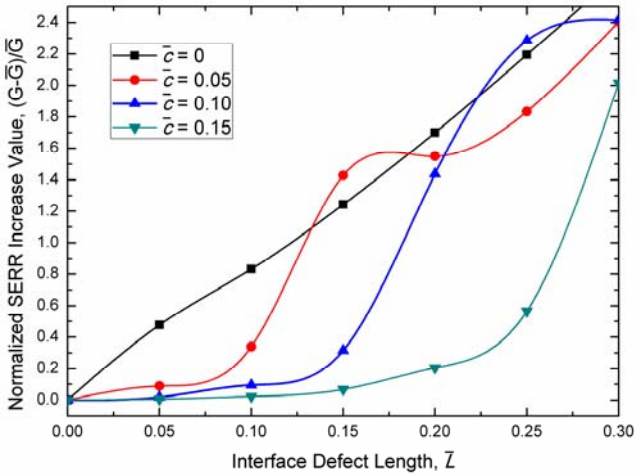

Figure 5. The maximum normalized SERR increment as a function of interfacial defect length and location.

4. Conclusions

The effects of interface defect on the surface fracture behavior of thermal barrier coating system (TBCs) are investigated in this work. The results show that the two important characteristic parameters, defect location and defect length, both have a significant influence on the driving force of surface crack. It is concluded a surface crack initiated above an interface defect propagates more easily since the enhancement of surface crack driving force is largest for the defect directly beneath the surface crack. Similarly, the surface crack propagates easier as the defect length increases. In present work, the critical value of the defect offset (below which the effect of an interface defect can be ignored) has been obtained and so does the critical value of defect length. By understanding the effect of the interface detect on the surface crack and using the critical value of the defect offset and defect length, the surface cracking behavior can be partially controlled. It is beneficial for

improving the durability of TBCs no matter by increasing the surface crack density to enlarge the strain tolerance of ceramic coating or reducing the surface crack to prolong the spalling of the ceramic coating.

Acknowledgements. This work is supported by the State 973 Program of China (2013CB035700), NSFC (11002104, 11021202, 11272259 and 11172227) and MOE fund.

References

[1] D. Clarke, C. Levi, Materials design for the next generation thermal barrier coatings. Annual review of materials research, 33 (2003) 383-417.
[2] R. Vaßen, M.O. Jarligo, T. Steinke, D.E. Mack, D. Stöver, Overview on advanced thermal barrier coatings. Surface and Coatings Technology, 205 (2010) 938-942.
[3] N.P. Padture, M. Gell, E.H. Jordan, Thermal barrier coatings for gas-turbine engine applications. Science, 296 (2002) 280.
[4] I. Zaplatynsky, Thermal expansion of some nickel and cobalt spinels and their solid solutions, National Aeronautics and Space Administration, 1971.
[5] T. Xu, S. Faulhaber, C. Mercer, M. Maloney, A. Evans, Observations and analyses of failure mechanisms in thermal barrier systems with two phase bond coats based on NiCoCrAlY. Acta materialia, 52 (2004) 1439-1450.
[6] Y.C. Zhou, T. Tonomori, A. Yoshida, L. Liu, G. Bignall, T. Hashida, Fracture characteristics of thermal barrier coatings after tensile and bending tests. Surface and Coatings Technology, 157 (2002) 118-127.
[7] A.G. Evans, D. Mumm, J. Hutchinson, G. Meier, F. Pettit, Mechanisms controlling the durability of thermal barrier coatings. Progress in Materials Science, 46 (2001) 505-553.
[8] W. Tie-Jun, Micro-and macroscopic damage and fracture behaviour of welding coarse grained heat affected zone of a low alloy steel: Mechanisms and modelling. Engineering Fracture Mechanics, 45 (1993) 799-812.
[9] G.W. Schulze, F. Erdogan, Periodic cracking of elastic coatings. International Journal of Solids and Structures, 35 (1998) 3615-3634.
[10] J.J. Vlassak, Channel cracking in thin films on substrates of finite thickness. International Journal of Fracture, 119 (2003) 299-323.
[11] X. Fan, W. Zhang, T. Wang, G. Liu, J. Zhang, Investigation on periodic cracking of elastic film/substrate system by the extended finite element method. Applied Surface Science, 257 (2011) 6718-6724.
[12] X.L. Fan, W.X. Zhang, T.J. Wang, Q. Sun, The effect of thermally grown oxide on multiple surface cracking in air plasma sprayed thermal barrier coating system. Surface and Coatings Technology, (2012).
[13] W. Zhang, X. Fan, T. Wang, The surface cracking behavior in air plasma sprayed thermal barrier coating system incorporating interface roughness effect. Applied Surface Science, (2011).
[14] J.R. Rice, Elastic fracture mechanics concepts for interfacial cracks. J. Appl. Mech.(Trans. ASME), 55 (1988) 98-103.
[15] D. Mumm, A. Evans, On the role of imperfections in the failure of a thermal barrier coating made by electron beam deposition. Acta materialia, 48 (2000) 1815-1827.
[16] D.L. Ruckle, Plasma-sprayed ceramic thermal barrier coatings for turbine vane platforms. Thin solid films, 73 (1980) 455-461.
[17] R.A. Miller, Current status of thermal barrier coatings--An overview* 1. Surface and Coatings Technology, 30 (1987) 1-11.
[18] Y. Bai, Z. Han, H. Li, C. Xu, Y. Xu, Z. Wang, C. Ding, J. Yang, High performance nanostructured ZrO2 based thermal barrier coatings deposited by high efficiency supersonic plasma

spraying. Applied Surface Science, (2011).
[19] O. Trunova, T. Beck, R. Herzog, R.W. Steinbrech, L. Singheiser, Damage mechanisms and lifetime behavior of plasma sprayed thermal barrier coating systems for gas turbines—Part I: Experiments. Surface and Coatings Technology, 202 (2008) 5027-5032.
[20] S.H. Song, P. Xiao, L.Q. Weng, Evaluation of microstructural evolution in thermal barrier coatings during thermal cycling using impedance spectroscopy. Journal of the European Ceramic Society, 25 (2005) 1167-1173.
[21] B. Zhou, K. Kokini, Effect of surface pre-crack morphology on the fracture of thermal barrier coatings under thermal shock. Acta materialia, 52 (2004) 4189-4197.
[22] X.L. Fan, R. Xu, W.X. Zhang, T.J. Wang, Effect of periodic surface cracks on the interfacial fracture of thermal barrier coating system. Applied Surface Science, 258 (2012) 9816-9823.
[23] J. Hutchinson, Z. Suo, Mixed mode cracking in layered materials. Advances in applied mechanics, 29 (1992) 191.
[24] J. Beuth, Cracking of thin bonded films in residual tension. International Journal of Solids and Structures, 29 (1992) 1657-1675.
[25] D. Dugdale, Yielding of steel sheets containing slits. Journal of the Mechanics and Physics of Solids, 8 (1960) 100-104.
[26] ABAQUS User's Manual, Dassault Systèmes Simulia Corporation, (2009).
[27] T.Y. Tsui, A.J. McKerrow, J.J. Vlassak, Constraint effects on thin film channel cracking behavior. Journal of materials research, 20 (2005) 2266-2273.
[28] M. Thouless, Z. Li, N. Douville, S. Takayama, Periodic cracking of films supported on compliant substrates. Journal of the Mechanics and Physics of Solids, (2011).